

ON THE FACTORIZATION AND ITS APPLICABILITY
IN WEAK NONLEPTONIC PROCESSES*

H. Galić[†]
Stanford Linear Accelerator Center
Stanford University, Stanford, California 94305

ABSTRACT

The role of the weak effective Hamiltonian in nonleptonic physics is studied. The application of the short-distance technique in simple pole transitions in mesons is justified. The amplitude, which is proportional to the matrix element of the Hamiltonian, is shown to be factorizable into a product of a coefficient function (hard part) and a matrix element of some local operator (soft part). The proof for such a factorization, valid to any order in the perturbative calculation is given. The problems encountered in the evaluation of soft parts are presented. The use of a similar procedure in more complicated weak transitions is questioned, and a discussion of the predictive power of the effective Hamiltonian approach is included.

Submitted to Physical Review D

* Work supported by the Department of Energy under contract number DE-AC03-76SF00515.

† On leave of absence from the Rudjer Bošković Institute, Zagreb, Croatia, Yugoslavia.

I. INTRODUCTION

In the last 25 years a number of experimental data on weak non-leptonic processes has been collected. On the other hand, until recently theorists have not been in a position to make valuable predictions in this field of physics. Their role was mainly restricted to looking for most natural explanations of various experimental facts. Even then the advance was slow and accompanied by difficulties. A typical example for such efforts is the chronology of the interpretation of the $\Delta I = \frac{1}{2}$ (or "octet") rule in $\Delta S = 1$ transitions. Experimental evidence for this selection rule by now is so strong that only the methods which provide an insight into the rule may securely be applied to other problems in weak nonleptonic physics. While the progress in the explanation of the rule has been achieved using arguments based on the current algebra, PCAC, and the color symmetries of hadron states (for baryonic transitions), there was no complementary interpretation of the octet dominance in terms of an effective interaction Hamiltonian.^{1,2}

The concept of the effective Hamiltonian was created in purely leptonic interactions. It is based on the observation that leptonic processes may be quite adequately described by a localized, current \times current type operator. A similar framework was traditionally used in the discussion of hadronic processes.¹ It was tacitly assumed that strong radiative corrections do not spoil the locality of the effective interaction, and the analysis of nonleptonic decays was carried out in terms of a local Hamiltonian. Although such an approach could qualitatively describe nonleptonic processes, the precise explanation of the $\Delta I = \frac{1}{2}$

selection rule was left to some unspecified strong-interaction dynamical effect.

The situation changed when Wilson³ suggested, in the context of the short-distance operator product expansion, a mechanism that could eventually acquire stronger short-distance singularities for $\Delta I = \frac{1}{2}$ than for $\Delta I = 3/2$ terms. Soon it was realized⁴ that the proper framework for the short-distance expansion is the asymptotically free theory of quantum chromodynamics (QCD). The fact that an ever increasing number of strong-interaction processes has been at least partially calculable using the operator expansion, raised the hope that something similar might be done even in a weak hadronic sector.

The pioneering works⁵ of Gaillard and Lee, and Altarelli and Maiani were quite successful. Not only was the class of QCD corrections to the $\Delta S = 1$, $\Delta C = 0$ weak Hamiltonian summed (with the help of the renormalization group (RG) equation), but also the desired result emerged: the octet part of the effective Hamiltonian was definitely enhanced. Although the effect was slightly too weak to account completely for the $\Delta I = \frac{1}{2}$ rule, a number of processes⁶⁻⁸ - including decays of newly discovered heavy mesons⁹, and CP-violating K-meson decays¹⁰ - have been analyzed since then¹¹ by the similar technique.

However, some caution concerning the applicability of the short-distance analysis in weak processes has been present all the time¹², due to the low-energy (i.e., long-distance) character of the considered weak decays. The argument that the exponential damping of the weak-boson propagator insures the dominance of short distances may be considered just as a heuristic one. It comes out that the "factorization" concept

provides a more natural framework for the discussion of the effective Hamiltonian and the influence of short distances on weak processes.

The procedure, similar to the one used in the straight QCD analysis,¹³ consists of two distinct steps. First, one must demonstrate that up to powers of the weak boson mass M (and eventually up to powers of heavy quark masses) the structure of momentum flows allows the weak amplitude to be factorized into a "soft" part (in which momenta are typically of the order of light quark masses), and a "hard" subprocess dominated by the large momentum ($\sim M$) flows. If such a factorization is possible, the soft part could be described in terms of hadronic matrix elements of renormalized local operators, whereas the hard part should be reduced to a coefficient function dependent on the large invariants solely. The next step then is the derivation of the RG equation for the coefficient functions.

While efforts in studies of weak decays were mostly restricted to the calculation of anomalous dimensions required in the RG analysis, little was done in the explicit justification of the first step.¹⁴ One indirect consequence of such a situation was the lack of a unique definition for the effective Hamiltonian, so that several different schemes may be traced in the current literature.¹⁶ In this work it is shown that no room for ambiguities is left when the correct approach is adopted. Although some freedom in the definition (due to the freedom in a choice of the renormalization and regularization scheme) remains, the form of the effective Hamiltonian is otherwise completely determined.

However, the main goal of the paper is to justify the short-distance technique and the use of the RG analysis in the evaluation of

the effective nonleptonic Hamiltonian. It is not a priori clear whether such an analysis can be carried out in some particular process or not.¹⁷ For each class of processes its application has to be verified explicitly. In subsequent sections the short-distance approach is justified for the broad scale of nonleptonic processes, to any order in the perturbative expansion. To complete the analysis, the discussion of the actual predictive power of the method is included.

The plan of the paper is as follows. In the next section the concept of the factorizability is introduced. In a one-loop example the conditions under which the W-boson mass dependence may be extracted from the amplitude by means of factorization will be examined. More precisely, the amplitude (which is proportional to the matrix element of the effective Hamiltonian) of a simple $\Delta S = 1$, $\Delta C = 1$ transition will be written as a coefficient function (which does not depend on the dynamics of the process) and of a matrix element of some local gauge-invariant operator. The entire M dependence is included in the coefficient function, and the matrix element is independent of the W-boson field. Note that only when such a factorization is exhibited, can the RG equation be used to determine the form of the coefficient function. In Sec. III, the analysis will be extended to a two-loop consideration. While the factorization in one-loop approximation is rather obvious, the higher order corrections require more careful treatment. In this section an explicit proof at the two-loop level is presented. Before the general proof of factorizability valid to any order in the perturbative calculation is given (in Sec. V), the $\Delta C = 0$, $\Delta S = 1$ and 0 , processes are considered in Sec. IV. Included is a discussion of the "second" factori-

zation. This tentative name is attributed to the procedure in which the dependence on the heavy quark masses is extracted from the amplitude. An immediate consequence of such an extraction is the appearance of new, "penguin" operators in the calculation. While the investigation in Sec. V definitely proves the factorizability in the sense given above, the disturbing problems discussed in Sec. VI do not give too many reasons for optimism: it is easy to see that the dependence of weak amplitudes on the heavy particle masses may be determined by the RG analysis, but the matrix elements of resulting operators still hide the completely uncalculable dependence on the light quark masses, dynamics and renormalization scheme. Therefore it is unlikely that more than a suggestive parametrization (in terms of unknown matrix element) is achieved. Any insistence on the precise numerical determination of actual nonleptonic amplitudes is not justified at present.

Although this paper should rather be considered as a kind of qualitative analysis, whenever necessary - especially in the proof of the factorizability - a detailed calculation is presented. In many other occasions the reader is referred to the existing literature on the subject. The standard, four-quark gauge model (with QCD, and electroweak coupling constants denoted by g and h , respectively) is used. However, the problems and conclusions would essentially be the same even in models with more than four flavors. The weak interactions are described in the renormalizable gauge.

II. FACTORIZABILITY IN $\Delta C = \Delta S = 1$ PROCESSES

In this and in the following section it is shown that the effective $\Delta S = 1$, $\Delta C = 1$ weak interaction may be factorized to a "hard" and "soft" part, in a class of processes in which the weak interaction takes place between two mesons. As an example, the virtual transition $D^0 \xrightarrow{\text{weak}} (\bar{K}^0)^*$ (followed in the physical process by strong two-body decay of the pole particle, $K^* \rightarrow K\pi$) is considered (see Fig. 1). The intention is to show that the effective weak Hamiltonian can be replaced by a set of local operators even when QCD corrections are taken into account. More precisely, it is claimed that the following equality is valid:

$$\langle K^* | \mathcal{H}_{\text{eff}} | D \rangle = \frac{1}{M^2} \sum_i C_i \langle K^* | \mathcal{O}_i | D \rangle + O(M^{-4}) \quad (2.1)$$

(M denotes the mass of the charged weak boson). The coefficients C_i in (2.1) are independent both on external states and dynamics of the process, and satisfy the RG equation.

Note that the evaluation of the amplitude (2.1) requires the knowledge of two important pieces of information. One is the probability of finding the proper quark-antiquark structure in the incoming (or outgoing) meson. This information should be built in wave functions of physical particles. In addition, the sum of all Born diagrams for $c + \bar{u} \xrightarrow{\text{weak}} s + \bar{d}$ scattering in the perturbative QCD has to be known. Just at this level the factorization should be demonstrated.

In what follows, the factorization will be explicitly proved to the order g^4 (two-loop level) by a careful diagrammatic analysis. In the

same manner an n-loop proof may (at least in principle) be formulated. However, a simpler (although more formal) general proof, based on the theory of the renormalization of operators, exists. It will be outlined in Sec. V.

It is important to emphasize that momenta of quarks inside mesons are in the further analysis considered to be much smaller than M and other large scales involved. (The term "short distances" should rather be associated with the large loop-momenta contribution, than with momenta of external particles). Therefore, the terms of order $1/M^4$ give small corrections, and - to simplify the notation - will often be omitted in further expressions.

At the quark level the relation (2.1) can be symbolically written as¹⁸

$$M^2 \langle \mathcal{H} \rangle_{0+2+4+\dots} = \left(C_i^0 + g^2 C_i^1 + g^4 C_i^2 + \dots \right) \langle \mathcal{O}_i \rangle_{0+2+4+\dots} \quad (2.2)$$

(The subscripts on $\langle \mathcal{H} \rangle$ and $\langle \mathcal{O}_i \rangle$ refer to orders of g contributions). The meaning of the above expression is as follows. The entire QCD corrections to the weak Hamiltonian can be factorized as a product of corrections to the coefficient function(s) and corrections to the matrix elements of the appropriate operator(s).

The inductive proof of the factorizability should include two steps; supposing that the relation (2.2) is valid to the order g^{2n-2} , one must show that

- (i) the order g^{2n} result is described by the same set of operators $\{ \mathcal{O}_i \}$,

$$M^2 \langle \mathcal{H} \rangle_{2n} = D_i^0 \langle \mathcal{O}_i \rangle_{2n} + g^2 D_i^1 \langle \mathcal{O}_i \rangle_{2n-2} + \dots + g^{2n} D_i^n \langle \mathcal{O}_i \rangle_0, \quad (2.3)$$

and that

(ii) the coefficients D_i satisfy relations

$$D_i^\ell = C_i^\ell \quad ; \quad \ell = 0, 1, \dots, (n-1), \quad (2.4)$$

i.e., coefficients remain the same as found by the lower order analysis.

(In addition, a new coefficient $D_i^n \equiv C_i^n$ is generated.) Only when both steps are confirmed, the inductive proof follows.

It is instructive to start the analysis with the consideration of the lowest order corrections to the process. They are presented in Fig. 2. One can show that to this order

$$\begin{aligned} \langle \mathcal{H} \rangle = & \frac{h^2 \cos^2 \theta}{8M^2} \left\{ \left(1 + \frac{g^2}{16\pi^2} A \right) (\bar{s}c)_{V-A} (\bar{u}d)_{V-A} \right. \\ & \left. + \frac{g^2}{16\pi^2} B (\bar{s}\lambda^a c)_{V-A} (\bar{u}\lambda^a d)_{V-A} \right\}, \end{aligned} \quad (2.5)$$

where

$$A = -\frac{1}{4} (\lambda^a \lambda^a) \int_0^1 2y dy \int_0^1 dx \ln \frac{\chi(x, y; m_\ell^2, p_i p_j)}{\chi_S}, \quad (2.6)$$

and

$$B = \frac{9}{4} - \frac{3}{2} \ln M^2 + \int_0^1 2y dy \int_0^1 dx \ln \phi(x, y; m_q^2, p_i p_j). \quad (2.7)$$

(A and B are contributions from Fig. 2a and 2b, respectively.) Functions χ and ϕ depend on the masses of quarks m_q , and external momenta p_j . The function χ_S in (2.6) denotes the contribution of the counterterm associated with the renormalization of the weak vertex in Fig. 2a. Its form depends on the procedure. For example,

$$\chi_S \equiv \chi(m_q, p_i p_j \sim -\mu^2) \quad \bar{\quad},$$

for the off-shell renormalization in a "symmetric point" μ^2 , and

$$\chi_S \equiv \chi(m_q \rightarrow 0, p_i p_j \sim -\sigma^2)$$

for the class of mass-independent renormalization schemes. One can - using the Fierz-rearrangement of both Lorentz and color indexes - reexpress (2.5) with the help of operators

$$\mathcal{O}_{84} = (\bar{s}c \bar{u}d + \bar{s}d \bar{u}c)_{(V-A)(V-A)} \quad (2.8)$$

$$\mathcal{O}_{20} = (\bar{s}c \bar{u}d - \bar{s}d \bar{u}c)_{(V-A)(V-A)}$$

transforming as components of 84 and 20 dimensional SU(4) representations. Equation (2.5) now reads

$$\begin{aligned} \langle \mathcal{H} \rangle = \frac{h^2 \cos^2 v}{8M^2} \frac{1}{2} \left\{ \left[1 + \frac{g^2}{16\pi^2} \left(A + \frac{2}{3} B \right) \right] \mathcal{O}_{84} \right. \\ \left. + \left[1 + \frac{g^2}{16\pi^2} \left(A - \frac{4}{3} B \right) \right] \mathcal{O}_{20} \right\} \quad . \end{aligned} \quad (2.9)$$

Operators in (2.9), due to their color, flavor and chiral structure are

candidates for the operator basis on the right-hand side of the expression (2.1). In order to show the validity of the relation (2.1), matrix elements of operators (2.8), i.e., the QCD corrections to the vertices generated by these operators, have to be found. The basic diagrams are displayed in Fig. 3. Since the diagrams are divergent, one must define the appropriate renormalization procedure in order to absorb divergences. When some of the known subtraction procedures are applied, the renormalized result can be written as

$$\begin{aligned} \langle \mathcal{O}_{84} \rangle_{0+2} &= \left[1 + \frac{g^2}{16\pi^2} \left(A + \frac{2}{3} \tilde{B} \right) \right] \mathcal{O}_{84} \\ \langle \mathcal{O}_{20} \rangle_{0+2} &= \left[1 + \frac{g^2}{16\pi^2} \left(A - \frac{4}{3} \tilde{B} \right) \right] \mathcal{O}_{20} \end{aligned} \quad (2.10)$$

where

$$\tilde{B} = \int_0^1 2y \, dy \int_0^1 dx \, \ln \frac{\phi(x, y; m_q^2, p_i, p_j)}{\phi_S} \quad (2.11)$$

ϕ_S (like χ_S in (2.6)) depends on the renormalization procedure.

Comparing expressions (2.5)-(2.7) and (2.9)-(2.11) one finds that

$$\langle \mathcal{H} \rangle_{0+2} = \frac{h^2 \cos^2 \theta}{8M^2} \frac{1}{2} \left\{ C_{84} \langle \mathcal{O}_{84} \rangle_{0+2} + C_{20} \langle \mathcal{O}_{20} \rangle_{0+2} \right\} \quad (2.12)$$

where

$$\begin{aligned} \begin{pmatrix} C_{84} \\ C_{20} \end{pmatrix} &= 1 + \frac{g^2}{16\pi^2} \begin{pmatrix} 2/3 \\ -4/3 \end{pmatrix} (B - \tilde{B}) \\ &= 1 + \frac{g^2}{16\pi^2} \begin{pmatrix} 2/3 \\ -4/3 \end{pmatrix} \left[\frac{9}{4} - \frac{3}{2} \ln M^2 + \iint \ln \phi_S \right] \end{aligned} \quad (2.13)$$

Thus, Eq. (2.1) is proved up to the order g^2 . The coefficients (2.13) are independent of dynamics and, for a suitable choice of the renormalization procedure, they do not even depend on the masses of quarks. Since coefficients (2.13) get their main contribution from the loop momenta of order M , they are sometimes referred to as a "hard" part of the effective Hamiltonian.

The method presented relies on an explicit evaluation of diagrams and obviously cannot be convenient for the higher orders proof. Another method, applied already to the short-distance analysis of $\Delta S = 2$ weak interactions by Witten,¹⁵ seems to be more helpful. It is based on a close correspondence between diagrams related to $\langle \mathcal{H} \rangle$ and $\langle \mathcal{O} \rangle$.

In general, two groups of diagrams are encountered in the evaluation of $\langle \mathcal{H} \rangle$. In the first group ultraviolet (UV) behavior allows the replacement of the weak boson propagator $(k^2 - M^2)^{-1}$ by $-1/M^2$, hence - in terms of graphs - allows the shrinkage of the propagator to a point. That can, for example, certainly be done for diagrams (x) and (a) in Fig. 2. The diagrammatic equality ($c \equiv \cos \theta$)

$$(2x) + (2a) = \frac{h^2 c^2}{8M^2} \left[(3x) + (3a) \right] (+O(M^{-4})) \quad (2.14)$$

is obvious. However, this procedure does not work when applied on diagrams 2(b). The shrinking of the weak propagator introduces an UV divergence in otherwise convergent integrals. (That is the consequence of the fact that M dependence of these diagrams is $(\ln M)/M^2$ rather than $1/M^2$, as may be seen from (2.7).) Fortunately, the differentiation with respect to external momenta improves the UV convergence. By simple power counting one can convince oneself that

$$\partial(2b) = \frac{\hbar^2 c^2}{8M^2} \partial(3b) \quad . \quad (2.15)$$

(The differentiation is symbolically denoted by ∂ .) After the integration, (2.15) becomes

$$(2b) = \frac{\hbar^2 c^2}{8M^2} \left[(3b) + \text{const.} \right] \quad . \quad (2.16)$$

The integration-constant term (proportional to g^2), since independent of momenta, must be a tree approximation matrix element¹⁵ of local operators (2.8). Combining (2.14)-(2.17) one gets (constant in (2.16) is denoted by $c_{(2)}$):

$$(2) = \frac{\hbar^2 c^2}{8M^2} \left[1 + g^2 c_{(2)} \right] \times (3) \quad . \quad (2.17)$$

This equality corresponds to the relation (2.12), derived earlier by a straight diagrammatic calculation.

In the same manner, the differentiation with respect to external momenta improves the UV behavior of higher order corrections, and helps to reach the step (i) in the inductive proof. Step (ii) could not be

verified at the one-loop level, and it might be interesting to check it explicitly in a two-loop calculation. The procedure, based on the combinatorics of diagrams, will be illustrated in the next section.

III. HIGHER ORDERS CONSIDERATION

While the passage from the tree approximation to the one-loop result is rather trivial, the extension to the two-loop level requires the justification of both steps (2.3) and (2.4), and may serve as a prototype for the general inductive proof.

To facilitate the writing, unimportant constants and indices are omitted, and symbolic "diagrammatic equations" are used. However, the careful treatment always stands behind such simplified notations.

It was already established, see Eq. (2.16), that diagrams in Fig. 2b differ from those in Fig. 3b by a constant, which turns out to be proportional to the tree approximation matrix element (3x):

$$(2b) = (3b) + g^2 c_{(2)} \times (3x) \quad . \quad (3.1)$$

A class of higher order corrections (CORR) to diagrams in Fig. 2b is presented in Fig. 4. Superficially, diagrams (2b) in a circle denoted in the figure may be replaced by the diagrams on the right-hand side of equation (3.1). But this expectation is false; the diagrams in Fig. 4, otherwise convergent, would become divergent, and the relation

$$\text{CORR } (2b) = \text{CORR} \left[(3b) + g^2 c_{(2)} \times (3x) \right] \quad , \quad (3.2)$$

is not correct. However, the differentiation with respect to external

momenta improves the convergence. It is explained in Fig. 5. If the derivative (marked with an X) acts on a propagator inside the subdiagram (2b) (as denoted symbolically in Fig. 5a), the boson propagator - as in Sec. II - can be replaced by $-1/M^2$:

$$\partial_{(a)} [\text{CORR}(2b)] = \partial_{(a)} [\text{CORR}(3b)] \quad . \quad (3.3)$$

When the derivative acts outside the subdiagram (as in Fig. 5b), the overall convergence is improved, but the convergence of the subdiagram is not. Therefore, the simple shrinking of the weak propagator is now forbidden. However, as demonstrated by Witten,¹⁵ the momenta that flow into the subdiagram (2b) become upon integration of the order of external momenta, and one may use the relation (3.1):

$$\partial_{(b)} [\text{CORR}(2b)] = \partial_{(b)} [\text{CORR}(3b)] + g^2 c_{(2)} \partial [\text{CORR}(3x)] \quad . \quad (3.4)$$

Equalities (3.3) and (3.4), summed and integrated, give the relation

$$\text{CORR}(2b) = \text{CORR}(3b) + g^2 c_{(2)} \text{CORR}(3x) + g^4 \bar{c}_{(4)}(3x) \quad , \quad (3.5)$$

which is now the correct form of (3.2). The last term in (3.5) is the integration constant. It is of the order g^4 , and represents the tree matrix element of the starting operator(s).

The simple power counting shows that all the other two-loop corrections either give g^4 contributions to the matrix element of operators (2.8), or add to the integration constant (thus changing $\bar{c}_{(4)}$ in (3.5) to $c_{(4)}$), but leave the middle term on the right-hand side of Eq. (3.5) unchanged. Since the corrections to the diagram (3x) are just the order

g^2 corrections to the matrix element of the starting operator(s),

$$\text{CORR}(3x) = \langle \mathcal{O} \rangle_2$$

one gets the final result

$$\langle \mathcal{H} \rangle_4 \sim \langle \mathcal{O} \rangle_4 + g^2 c_{(2)} \langle \mathcal{O} \rangle_2 + g^4 c_{(4)} \langle \mathcal{O} \rangle_0 \quad . \quad (3.6)$$

As expected, $c_{(2)}$ is the same constant as already found in Sec. II.

Any other outcome would mean that the factorization does not exist.

The elements of the analysis just described, may be of use in a general inductive proof. The differentiation improves the convergence of any n-loop diagram. It is illustrated in Fig. 6. The position of the differentiation mark determines what should be considered as a subdiagram. As before, when the derivative acts on the "external leg" of the subdiagram (for which, by the assumption, (2.2) has already been shown), the subdiagram becomes dominated by loop momenta of the same order as external momenta. That enables one to express the subdiagram as a linear combination of matrix elements of local operators (see Fig. 6). The integration-constant term (independent on external momenta) is - due to the chiral, color and flavor structure - the tree matrix element of the starting operator(s), and no new operators enter the analysis. That completes part (i) of the inductive proof. The proof of step (ii) requires the careful sorting of n-loop diagrams: in the first group "simple" corrections to the (n-1)-loop Hamiltonian have to be classified. (Corrections analogous to those in Fig. 4 are called "simple"). For this class, just as in the two-loop calculation, one should get

$$\begin{aligned} \text{CORR}\langle\mathcal{H}\rangle_{2n-2} &= \text{CORR}\langle\mathcal{O}\rangle_{2n-2} + \text{CORR}\left[g^2 c_{(2)}\langle\mathcal{O}\rangle_{2n-4} + \dots\right] \\ &+ g^{2n}(\text{const.}) \times \langle\mathcal{O}\rangle_0 \quad . \end{aligned} \quad (3.7)$$

All other n-loop corrections should contribute either to the first, or to the last term on the right-hand side of (3.7), not affecting the remaining part of the expression.

Note, by the way, that through a similar analysis one may show a factorizability of the electromagnetic corrections to weak $\Delta S = \Delta C = 1$ processes. The factorizability, as far as weak interactions are considered, has nothing to do with the specific asymptotic behavior of the QCD (or QED), but is rather the consequence of the renormalizability.¹⁹

The rough sketch given above just indicates the path which could be followed by the actual proof. In reality the proof of step (ii) becomes extremely complicated due to the variety of corrections that have to be taken into account when the number of loops exceeds two or three. To circumvent these difficulties a completely different method is used in Sec. V, in the general proof of the factorizability. However, the technique presented in the preceding and this section has the advantage that one can visualize what is actually done in the calculation: a weak interaction problem (the evaluation of $\langle\mathcal{H}\rangle$) is transformed into the "pure" QCD problem (the calculation of matrix elements $\langle\mathcal{O}\rangle$). The weak interactions have left their trace in the chiral and flavor structure of operators, but the W-boson field is completely eliminated. Only the mass of the weak boson appears as an argument upon the value of which the coefficient functions C_i depend.

One might wonder what the main goal of such a procedure is. The situation is not analogous to that encountered in the application of the short-distance technique in straight QCD.¹³ There, in the class of reactions at large transverse momentum q^2 the dynamics of the (hard) scattering process can be factorized from the physics of the hadronic wave function. Thus the ratio of two quantities measured at different energies does not depend on bound state dynamics and on the precise evaluation of the matrix elements (the soft part at both energies is the same). The characteristic example is the description of the pion form factor at large q^2 . In few cases not only the hard part, but also hadronic wave functions can be treated perturbatively.¹³ In weak processes matrix elements cannot be calculated and the W-boson mass - that plays a role of (large) q^2 - is fixed, there is no possibility for the comparison, and the soft part cannot be removed. Although the M^2 -dependence of the coefficients can be found, as long as the QCD corrections to the operator vertices are uncalculable, nothing but a suitable parametrization is achieved. Such parametrization may have sense only if the matrix elements of various operators are expected to be of the same order of magnitude. Then, by comparing coefficients, the relative importance of operators with diverse substructure (e.g., $\Delta I = 0$ and 1 isospin changing operators), contributing to a single process, can be determined. Otherwise, the further improvement of the analysis must be looked for. The processes in which an approximate equality of matrix elements of operators is not expected, are studied in the next section.

IV. $\Delta C = 0$ PROCESSES - "SECOND" FACTORIZATION

As far as the elimination of the W-boson field is considered, the analysis of the factorizability for the $\Delta S = 1$, $\Delta C = 0$ processes does not differ much from the analysis in the preceding section. However, while in the $\Delta C = 1$ case the exchange of the weak boson always happens between two quark-lines, in the $\Delta C = 0$ processes the weak transition may occur even in a single quark-line. Nevertheless, as will be shown, the operator basis remains similar to those found in the previous case, and is constructed by only two operators.

The discussion is again restricted to virtual weak decays in the meson sector. The particular process to be considered is the $(K^0)^* \rightarrow \pi^+ \pi^-$ transition, the weak part of the $K^0 \rightarrow \pi^+ \pi^-$ decay displayed in Fig. 7.

The free-field result (no QCD corrections) can be described with the help of two operators related by their SU(4) properties to operators (2.8):

$$\begin{aligned} \mathcal{O}_{84} &= \left[(\bar{d}u\bar{u}s - \bar{d}c\bar{c}s) + (\bar{d}s\bar{u}u - \bar{d}s\bar{c}c) \right]_{(V-A)(V-A)} \\ \mathcal{O}_{20} &= \left[(\bar{d}u\bar{u}s - \bar{d}c\bar{c}s) - (\bar{d}s\bar{u}u - \bar{d}s\bar{c}c) \right]_{(V-A)(V-A)} \end{aligned} \quad (4.1)$$

When higher order corrections are taken into account, a set of diagrams which have no precedents in Sec. II and III, may be constructed⁷ (see Fig. 8). Such new "penguin" diagrams might create a new set of local operators (penguin operators) not included in (4.1). However, as a consequence of the renormalizability, such a situation does not occur: the entire contribution of penguin diagrams (in which the weak transition

takes place in a single quark-line) may be absorbed into the matrix elements of operators (4.1), and no new operator is needed in the basis.

To illustrate this statement let me first consider the diagram in Fig. 9. (The degree of divergence for such a "self-energy" diagram is so high that even the Higgs ghost particle ϕ contributes to the order $O(1/M^2)$.) To the lowest order, the $s \rightarrow d$ transition is described by the unrenormalized amplitude ($s \equiv \sin\theta$)

$$\begin{aligned} \mathcal{M}_{d\partial s} &\sim \frac{h^2_{sc}}{8M^2} (m_u^2 - m_c^2) \left[-\frac{2}{n-4} + \text{const.} - \ln M^2 \right] \\ &\times \bar{d}\not{p}(1 - \gamma_5)s + O(M^{-4}) \end{aligned} \quad (4.2)$$

The residue at the pole $n \rightarrow 4$ is proportional to $(m_u^2 - m_c^2)/M^2$, and no mass-independent renormalization scheme exists for the weak interaction part of the standard model. However, the renormalization constant can be defined as the value of the expression (4.2) calculated at some fixed external momenta. Since the interesting part of (4.2) is independent of momenta, the entire $1/M^2$ contribution of Fig. 9 is absorbed into the (weak) renormalization constant

$$Z_{d\partial s} \sim \frac{h^2_{sc}}{8M^2} (m_u^2 - m_c^2) \left[-\frac{2}{n-4} + \text{const.} - \ln M^2 \right], \quad (4.3)$$

and diagrams 9 (and 8a) do not contribute to $\langle \pi | \mathcal{H} | K^* \rangle$.

Another interesting diagram is presented in Fig. 10. While the $\bar{d}sG$ part of this vertex correction is absorbed by the renormalization constant (4.3), the remainder deserves attention. The appropriate

matrix element, up to $1/M^2$ terms, is

$$\begin{aligned} \mathcal{M}_{ds\partial\partial G} &\sim \frac{h^2_{sc}}{8M^2} \int_0^1 dx \, x(1-x) \ln \frac{m_u^2 - q^2 x(1-x)}{m_c^2 - q^2 x(1-x)} \\ &\times \frac{g}{4\pi^2} \bar{d}\gamma_\alpha (1-\gamma_5) \lambda^a_s (q^\alpha q^\beta - g^{\alpha\beta} q^2) G_{\underline{\beta}}^a + O(M^{-4}) \end{aligned} \quad (4.4)$$

However, the result (4.4) does not have $\ln M^2$ dependence, and that means that weak propagators in Fig. 10 can be shrunk to a point. In other words, diagrams 10 (and 8b) do not generate new operators, but rather contribute to matrix elements of starting operators (4.1), as indicated in Fig. 11. This property is the consequence of the GIM mechanism and of the renormalizability (the dimension-six counterterm, $\bar{d}s\partial\partial G$, is forbidden in the renormalizable Lagrangian), and hence it must be fulfilled to any loop level (see the related discussion in Ref. 20).

Once the possible source of new operators is eliminated, the analysis proceeds just as in Sec. II and III. The contribution of standard diagrams (analogous to those in Fig. 2) may be factorized, leading to the effective $\Delta S = 1$, $\Delta C = 0$ Hamiltonian of the form

$$\langle \mathcal{H} \rangle = \frac{h^2_{sc}}{8M^2} \frac{1}{2} \left\{ c_{84} \langle \mathcal{O} \rangle_{84} + c_{20} \langle \mathcal{O} \rangle_{20} \right\} \quad (4.5)$$

The coefficients C are the same as in (2.13). Like in the $\Delta S = \Delta C = 1$ case, the factorization is true for any choice of both the renormalization scheme, and the renormalization scale.

So far, the amplitude of the weak process is parametrized by two,

generally unknown, matrix elements

$$\langle \mathcal{O}_{84} \rangle \text{ and } \langle \mathcal{O}_{20} \rangle . \quad (4.6)$$

However, looking back on diagrams that determine (4.6), one finds two clearly distinctive classes: diagrams without (similar to those in Figs. 3a,b), and with (see Fig. 11b) closed fermion loops. The former "standard" diagrams are expected to maintain the original left-left chiral structure, but the latter - due to vector coupling of the gluon field - must in addition have left-right parts too. Since mesons contain both left- and right-handed quarks, it is expected that diagrams with closed loops (being able to annihilate both components of the meson wave function) have an important role in the description of the process. Therefore, one would like to separate their contribution. According to the decoupling theorem,²¹ it may be done in certain circumstances.

More precisely, if none of the external particles is the charm-quark, and if external momenta may be considered small as compared to m_c , the matrix elements (4.6) can be further factorized

$$\langle \mathcal{O}_i \rangle \sim \sum D_{ij} \langle \mathcal{P}_j \rangle \left(+ O(m_c^{-2}) \right) , \quad (4.7)$$

where the new operator basis $\{ \mathcal{P}_j \}$ belongs to the "effective field theory",^{15,21} with only three quark flavors. The method is described extensively in the literature^{7,10,15} and here only the main idea will be illustrated.

The goal of the second factorization (4.7) is explained earlier: two parameters (4.6) are replaced by a larger number of unknown matrix

elements $\langle \mathcal{P}_j \rangle$, but with the expectation that in the new basis hopefully dominant penguin operators will appear explicitly.

The factorization (4.7) is almost evident for the "standard" diagrams, and the discussion will be concentrated on the contribution of the diagram 11b. It is easy to get (in the four-flavor theory!)

$$\begin{aligned} \langle \mathcal{O}_{84,20} \rangle_{\text{Fig. 11b}} &\sim g^2 \int_0^1 dx x(1-x) \ln \frac{m_u^2 - q^2 x(1-x)}{m_c^2 - q^2 x(1-x)} \\ &\times \frac{1}{4\pi^2} \bar{d} \gamma_\alpha (1 - \gamma_5) \lambda^a_s \bar{u} \gamma^\alpha \lambda^a_u \quad . \end{aligned} \quad (4.8)$$

The integral in (4.8) can be rearranged to read

$$\begin{aligned} &\int_0^1 dx x(1-x) \ln \frac{\tau_S}{m_c^2} \\ &+ g^2 \int_0^1 dx x(1-x) \ln \frac{m_u^2 - q^2 x(1-x)}{\tau_S} + O(m_c^{-2}) \quad , \end{aligned} \quad (4.9)$$

where τ_S is some constant (independent of external momenta), the interpretation of which will become clear in the following. The first term in the decomposition (4.9) may be considered as an order- g^2 correction to the (m_c -dependent) coefficient function D in (4.7), and the second term as an appropriately renormalized g^2 correction to the matrix element of operators

$$(\bar{s}u\bar{u}d \pm \bar{s}d\bar{u}u)_{(V-A)(V-A)} \quad , \quad (4.10)$$

in a theory with only three quark flavors. In such an interpretation τ_S characterizes the renormalization scheme. Like ϕ_S and χ_S before (see Sec. II), τ_S may be either dependent, or independent on masses of (light) quarks.

The appearance of the renormalization function τ_S implicitly signals the presence of the new component in the basis of ~~renormalized~~ operators. The new term has a form [see (4.8) and (4.9)] characteristic for penguin operators:

$$(\bar{d}\lambda s)_{V-A}(\bar{u}\lambda u)_V \quad . \quad (4.11)$$

Note that the elimination of the charm-quark field in the course of the second factorization made the GIM mechanism inoperable, and penguin diagrams (Fig. 11) divergent. Consequently, new counterterms had to be introduced (or in other words, new operators were admixed) in the renormalization procedure, and the goal of the second factorization was achieved: penguin operators (4.11) emerged explicitly in the basis $\{\mathcal{P}\}$.

Higher order contributions to $\Delta S = 1$, $\Delta C = 0$ processes will be discussed in context of the general proof of the factorizability, in the next section, and this section will be concluded with a brief analysis of the $\Delta S = 0$, $\Delta C = 0$ weak interactions.

The new feature is that even the neutral currents can contribute to $\Delta S = \Delta C = 0$ processes, considerably increasing the operator basis already in the free-field limit.⁶ In addition to 84 and 20 terms, the basis contains operators transforming as 15- and 1-dimensional representations. Furthermore, due to the fact that neutral currents in the

standard model are coupled to the left- as well as to the right-handed quarks, the operators with mixed left-right chirality emerge even before the QCD corrections are introduced. That affects substantially the higher order calculation. For example, at the one-loop level the leading contribution of the penguin-like diagrams in Fig. 12 is not of the order $1/M^2$ [compare with (4.4)], but of the order $(\ln M^2)/M^2$. Thus the shrinking of weak propagators is forbidden, and diagrams in Fig. 12 must be related to matrix elements of the new, penguin operator (compare with the different situation in Fig. 11). In other words, already the extraction of the weak boson masses introduces the penguin operators in the effective Hamiltonian. (In the previous example those operators appeared only when the charm-quark mass was extracted from the amplitude.)

From the technical point of view the analysis becomes extremely involved, but no new concepts are required and the procedure suggested throughout this work suffices for the proof of the factorizability even in this case.

V. GENERAL PROOF OF FACTORIZABILITY

The "diagrammatic" analysis given in previous sections raised a hope that the factorization might really be done for weak transitions discussed so far. Furthermore, throughout the analysis the very concept of the effective interaction became more plausible and understandable. The same technique will therefore serve in the next section as the basis for the discussion on the applicability of the factorization in non-leptonic processes. However, one must be aware of problems arising

when an attempt is made to transmute the sketch of the inductive proof, given at the end of Sec. III, to the rigorous and general proof. In order to circumvent difficulties, another method will be used in this section. It is based on the close relationship between the theory of the renormalization of operators²² (TRO), and the factorizability. Since the TRO is already known to be valid to any-loop order, such an approach seems to be more convenient for a general proof.

It is useful to start the analysis by forgetting weak interactions for a moment, and concentrating the attention to the straight QCD problem of the renormalization of operators. The objects under consideration in a TRO are Green's functions involving insertions of operators. In general an operator will mix with other operators in a renormalization procedure. However, a simpler example of multiplicatively renormalizable operators [such as operators (2.8)] suffices for the purpose of the introductory discussion.

To remove the divergences in Green's functions (GF) of some operator, one has to add counterterms to the Lagrangian in such a way that counterterms cancel poles in GF.²² As far as GF with only one insertion of a multiplicatively renormalizable operator are considered, the TRO proves to any loop order that one and only one counterterm is needed.

Furthermore, the right regularization procedure - which isolates the infinities appearing in individual diagrams - has to be chosen. In principle, any regularization, as long as it preserves the gauge symmetries of the theory, may be adopted. The suitable choice of the regularization will be the main step in the following proof.

The basic source of interesting divergences (i.e., of divergences

that cannot be removed by the QCD renormalization of fields and coupling constants) is the vertex in which an operator is placed. To be more concrete, operators (2.8) are examined. The Feynman rule for the vertex corresponding to one of the operators in (2.8) is typically of the form

$$\left\{ \gamma_{\mu} (1 - \gamma_5) \right\}_{1-2} \left\{ \gamma^{\mu} (1 - \gamma_5) \right\}_{3-4} \quad , \quad (5.1)$$

where indices denote quark-lines along which the vertex has to be read. Let me now consider diagrams in which (5.1) is replaced by the following non-local vertex:

$$-\Lambda^2 \left\{ \gamma_{\mu} (1 - \gamma_5) \right\}_{1-2} \left\{ \gamma^{\mu} (1 - \gamma_5) \right\}_{3-4} \frac{1}{q^2 - \Lambda^2} \quad . \quad (5.2)$$

Here Λ is some parameter, and q is the momentum flowing through the vertex from quark lines 1-2 to lines 3-4. (In general q is the function of external as well as of loop momenta.) For small values of q^2 , vertex (5.2) exhibits the same behavior as vertex (5.1), but when q^2 grows and becomes larger than Λ^2 , the expression (5.2) turns off. On the other hand, as $\Lambda^2 \rightarrow \infty$, the original UV divergence is rediscovered. Then it follows that Λ in (5.2) is the regularization parameter which plays a role of a UV cutoff.

In the actual theory, only the diagrams with the vertex (5.1) appear. However, through the regularization procedure, to any diagram with the vertex (5.1) another diagram with the vertex (5.2) may be related. That is illustrated in Fig. 13. In Fig. 14, the statement of the renormalizability is explained: the divergent part (when $\Lambda \rightarrow \infty$) of diagrams on the left-hand side of the picture can be isolated in a

constant multiplying the remaining, finite, Λ -independent part.

Figure 15 illustrates the crucial step in the proof. One considers a regularized vertex for the sum of operators \mathcal{O}_{84} and \mathcal{O}_{20} ,

$$\mathcal{O} = \frac{1}{2} (\mathcal{O}_{84} + \mathcal{O}_{20}) = \bar{s}c\bar{u}d_{(V-A)(V-A)} \quad (5.3)$$

It is easy to see that the regularized vertex corresponding to the operator (5.3) describes exactly the $\Delta S = \Delta C = 1$ interactions in a theory with a weak boson of mass Λ . Consequently, the right-hand side of Fig. 15 corresponds to $\langle \mathcal{H}_{\Delta S = \Delta C = 1} \rangle$, provided that Λ is replaced by M . By comparison of Figs. 13, 14 and 15, the following relation can be derived:

$$\begin{aligned} M^2 \langle \mathcal{H} \rangle_{M^2, (p_i p_j)} &\sim Z_{84}^{-1}(M^2) \times \text{ren} \langle \mathcal{O}_{84} \rangle_{(p_i p_j)} \\ &+ Z_{20}^{-1}(M^2) \times \text{ren} \langle \mathcal{O}_{20} \rangle_{(p_i p_j)} + O(M^{-2}) \end{aligned} \quad (5.4)$$

Note again that the left-hand side of the relation (5.4) represents properly regularized (with a "cutoff" $\Lambda = M$), but unrenormalized four-quark 1PI Green's function with the insertion of the operator (5.3). However, the relation (5.4) is just the required proof of the factorizability: matrix elements of the effective Hamiltonian are written in the operator basis (2.8). While the similar result has already been derived at the two-loop level [compare with (3.6)], the factorization (5.4) is now valid, according to the TRO, to any loop order in the perturbation theory.

To summarize, the renormalization of two particular gauge invariant

operators listed in (2.8) is considered. The insertion of an operator in a GF creates divergences, yet a well-defined procedure of the renormalization exists.²² In order to deal with divergent quantities, a procedure relating finite (but procedure dependent) expressions to all infinite quantities is established. This regularization procedure is selected very carefully: it is designed in such a way that it reproduces the original divergences when the regularization parameter tends to infinity, but imitates the weak interaction theory when the parameter takes a finite value of the weak boson mass. Thus, GF with operator insertions are in a unique manner related to GF with a (single) W-boson exchange. However, the matrix elements of the effective Hamiltonian may be expressed with the help of such GF, and one finally finds that $\langle \mathcal{H} \rangle$ can be factorized in the operator basis $\{O_{84}, O_{20}\}$. Moreover, the factorization coefficients correspond to renormalization constants of operators evaluated at the finite value $\Lambda = M$.

Let me now consider the $\Delta S = 1$, $\Delta C = 0$ transitions. The first step in the proof of the factorizability for these transitions is as simple as it was for the $\Delta S = \Delta C = 1$ processes. The new feature, however, appears when the next step - the second factorization - is examined. Let me remind the reader that the goal of the second factorization is to reexpress the matrix elements of certain operators in the four-flavor theory, with the help of an operator basis in the three-flavor theory. In the sense of the previous discussion, first the renormalization of operators in the QCD with only three flavors has to be analyzed. Interesting operators are those mixing with the operator (4.10) in the renormalization procedure.

It turns out that (quadratically divergent) diagrams with closed quark loops, created by (4.10), remain divergent even after the operator vertex is rearranged according to (5.2). (See Fig. 16. For simplicity, the procedure is illustrated at the one-loop level.) Therefore another regularization parameter has to be introduced. The purpose is the same as before - to choose the regularization scheme in such a way that, to a certain limit, the underlying weak theory emerges explicitly. The following procedure fulfills this requirement: the u-quark propagators appearing in a diagram with a closed quark loop originated from the operator (4.10) have to be replaced throughout the regularization procedure, according to the instruction

$$\prod_i (\not{p}_i - m_u)^{-1} \rightarrow \prod_i (\not{p}_i - m_u)^{-1} - \prod_i (\not{p}_i - \rho)^{-1} . \quad (5.5)$$

Here p_i is the momentum flowing through the i-th fragment of the up-quark loop (in general, p_i is a function of external and loop momenta), while ρ is the new regularization parameter. It is clear that the $\rho \rightarrow \infty$ limit reproduces the original divergences of the three-flavor theory. However, for any finite value of the regularization parameter, (5.5) is nothing but the "GIM mechanism" in the four-quark model with the heavy quark of the mass ρ . A simple combinatorics now leads to the proof of the second factorizability (4.7): matrix elements (4.6) may be reexpressed (to the accuracy $1/m_c^2$) in the three-flavor operator basis, to any given order in the perturbation theory.

So far, it was tacitly assumed that the selected regularization procedure preserved the global and local gauge symmetries. One intuitive-

ly feels that such an assumption is justified, at least to the leading order in M and m_c : the regularization is chosen in such a way that the features of the standard electroweak theory, known to obey the gauge-invariance, are imitated.

In this section the factorizability (including the "second" one) has been proved to any loop-order. However, the more formal character of the proof has pushed the real physical problems into the background. As already mentioned, the discussion on the applicability in the next section is based on the "more physical" diagrammatic approach adopted in Secs. II - IV.

VI. CRITICAL LOOK ON THE APPLICATION

In the preceding sections several weak virtual transitions in mesons were discussed. It was shown that the processes really exhibited specific short-distance behavior, and that the factorization could be carried out. Once the factorizability is proven (and only then), it is quite easy to show that coefficient functions satisfy a renormalization group equation. For example, the coefficients C_i ($i = 8, 4, 20$) in (2.12) and (4.5) obey, in a mass-independent renormalization scheme, the equation

$$\left[\sigma \frac{\partial}{\partial \sigma} + \beta(g) \frac{\partial}{\partial g} - \gamma_i(g) \right] C_i(M/\sigma, g) = 0 \quad , \quad (6.1)$$

for any value of the parameter σ (the "renormalization point"). However, the mass-independent scheme is not the unique choice. For some other renormalization procedure the additional terms might appear in (6.1) and

the RG equation would have different form and solutions. Yet the differences in C_i are compensated for by the differences emerging in the calculation of the matrix elements of operators. In principle Eq. (6.1) may be solved to any order of accuracy. (In reality the calculation is mostly restricted to the leading logarithmic approximation. See, however, Ref. 23.) Therefore, the coefficients C_i [and D_i - see Eq. (4.7)] are from now on treated as known, and attention will be concentrated on the matrix elements.

In the course of this paper it was emphasized that by doing factorization the main problem of the analysis was shifted from the weak interactions to the straight QCD regime. A certain class of radiative corrections to the W-boson exchange was summed, but strong corrections related to the vertices generated by operators remained undetermined. This problem was already known to the authors of the pioneering works on the subject. However, the progress in the description of hadrons by quark-model wave functions turned suspicion into hope. Indeed, considerable success in accounting for many properties of hadrons (in particular static) was achieved in this framework.^{24,25} Therefore it might seem that the quark wave functions provide the solution to the problem of calculation of operator matrix elements. Yet at present their application in nonleptonic physics seems to be justified only in rough estimates and one still does not have a suitable basis for precise numerical calculations. This conclusion emerges from the following observation. While the real matrix elements crucially depend on both the renormalization parameter and the renormalization procedure, the accessible wave functions (for example in the bag²⁴ - or in the harmonic oscillator -

model²⁵) are totally insensitive on the variation of those elements. Arguments that some choice of the procedure might describe the physics more adequately than some other, have by now no solid confirmation. It is hard to imagine any substantial progress before the renormalization dependence is built in the wave functions.

Up to this point simple, virtual, two-body meson transitions have been considered. The problems concerning the calculation become even more significant when more complicated transitions are taken into account. One example is displayed in Fig. 17. The factorization may again be achieved by the method used in previous sections. However, not only the renormalization procedure dependence, but the momentum and light quark mass dependence, and even the chiral and color structure of the expression in square brackets (Fig. 17) remain now unknown. (The analogous problems are encountered in the analyses of the three-body meson and baryon decays; see for an example Fig. 18.) In all such transitions a four-quark operator is "forced" to describe a process in which six or more quarks take place. The approximation in which the quark not interacting with the weak boson is considered as a mere "spectator" might help to lessen the problem, however, new data (especially for the D-meson decays) cast considerable doubt² on this popular approach.

Let me look at another aspect of the problem. The "direct" application of the weak Hamiltonian is by no means the only way by which the nonleptonic decays in terms of the effective interaction are treated. While the considered virtual transitions represent the so-called pole contribution, at least two other distinctive types of theoretical contributions can be isolated. The first one is based on the current

algebra analysis.¹ By reducing the pion field via PCAC in a process $A \rightarrow B + \pi$ one is left with the rotated Hamiltonian between states A and B. Schematically

$$\langle B\pi | \mathcal{H} | A \rangle \rightarrow \text{const.} \times \langle B | \tilde{\mathcal{H}} | A \rangle \quad . \quad (6.2)$$

Thus a matrix element of the Hamiltonian between baryon (or meson) states emerges and the analysis corresponds to the analysis of the pole contributions (Secs. II - V).

Another type of contribution is related to the operator structure of the effective Hamiltonian. It is the "separable" contribution,⁷ following from the assumption that the four-quark operator can be written as a product of two quantities ("currents") bilinear in quark fields. For example, if the operator $\mathcal{O} = (\bar{a}b)(\bar{c}d)$ contributes (via an effective Hamiltonian) to a transition $A \rightarrow B + \pi$, the assumption is that the separation

$$\langle B\pi | \mathcal{O} | A \rangle \sim \langle B | (\bar{a}b) | A \rangle \langle \pi | (\bar{c}d) | 0 \rangle \quad (6.3)$$

can be done. The assumption (6.3) bears far-reaching consequences. Namely, as shown elsewhere,^{7,8,10} without separable contributions [based on (6.3)] it is almost impossible to describe successfully the decays of the kaon and hyperons. Therefore, it is worthwhile to examine how the assumption (6.3) fits the factorization picture developed by now.

Let me remind the reader on the meaning of brackets around an operator in a factorized result. $\langle \mathcal{O} \rangle$ denotes the renormalized contribution of all-order QCD radiative corrections to the vertex generated by the operator \mathcal{O} . That means that $\langle \mathcal{O} \rangle$ carries the information on the

subtraction scheme used in the course of the renormalization. Imagine now that the operator may be written as a product of two other operators, $\mathcal{O} = \mathcal{P} \cdot \mathcal{R}$. Let me consider the product

$$\langle \mathcal{P} \rangle \langle \mathcal{R} \rangle \quad . \quad (6.4)$$

Each operator in (6.4) has now its own renormalization-procedure subtraction scheme. Even more, these schemes are completely unrelated to the scheme used in the evaluation of $\langle \mathcal{O} \rangle$. This fact can be represented pictorially. In general the diagram in Fig. 19 cannot be cut through the operator vertex. Vertices on the right-hand side acquire, by the renormalization, the counterterms which cannot be brought into relation with the counterterm belonging to the operator \mathcal{O} on the left-hand side. It must be concluded that the separation (6.3) might easily be ill-defined. In other words, (6.3) is correct just to some level of approximation. The gluon corrections that "bridge" the operator (as the one in Fig. 19) are of the greatest importance in the estimate of the validity of the separation (6.3). The more important these corrections are, the less confident the relation (6.3) is. Unfortunately, no real attempt to elucidate this problem has been described so far in the literature.²⁶

VII. CONCLUSION

An increasing number of papers using the effective weak Hamiltonian and the short-distance technique in calculations of nonleptonic decay rates, of both mesons and baryons, has intensified the necessity for an explicit proof of the factorizability. The main part of the present

paper is addressed to this problem, and the proof valid to any order is achieved. By the same method it is easy to prove that the factorization (as far as under this name the isolation of the W-boson and heavy quark masses from the amplitude is considered) may be done even for more complicated non-valence Fock states (i.e., $q\bar{q}G$, $qqq\bar{q}$, ...) of mesons and baryons.

Despite this attractive feature, the problem of applicability still seems to be far from the solution. The part of QCD corrections in the amplitude can be definitely summed and incorporated into the coefficients of the operators; but at present there is no way to take into account the remaining corrections confined in the matrix elements of operators. The analyses exploring the quark-model wave functions may be used in a rough estimate of the matrix elements, but a more pretentious application does not seem to be justified. A suggestive parametrization is achieved by the factorization, but that sheds little light on the problem: as long as more reliable wave functions sensitive on the details of the renormalization procedure are not accessible, the predictive power will be small. Presumably, the ability to produce more realistic wave functions will be improved with time. In the mean time an immediate application of the concept of the effective Hamiltonian might be tried in a calculation depending more on experimental data. One should investigate and understand more properly the reliability and the range of applicability of the separation indicated in (6.3). Then, if such a separation proves reasonable, the unknown matrix elements of operators and the measured (rather than calculated) weak formfactors could be brought into relation, and the semiempirical calculation might be feasible.

Another possibility is that a completely new approach, not necessarily based on the effective Hamiltonian, should be devised.²⁷ Anyhow, the optimism regarding the understanding of the $\Delta I = \frac{1}{2}$ rule, and - more generally - the calculability of nonleptonic amplitudes in terms of the operator expansion, seems to be premature. There is still a lot to be done before an ultimate and successful concept emerges.

ACKNOWLEDGMENT

I have benefited greatly from discussions with S. Gupta. I would also like to thank S. Brodsky and H. Quinn for their helpful comments. This work was supported by the Department of Energy, under contract number DE-AC03-76SF00515.

REFERENCES

1. R. E. Marshak, Riazuddin and C. P. Ryan, Theory of Weak Interactions in Particle Physics, (Wiley, New York, 1969).
2. For recent reviews see, for example, R. D. Peccei, Lectures at 17th Karpacz Winter School, Karpacz, Poland, February 1980, and MPI-PAE/PTh 6/80 (April 1980) unpublished; S. Pakvasa, Talk at 20th Int. Conf. on High Energy Physics, Madison, Wisconsin, July 1980, and UH-511-410-80 (September 1980) unpublished.
3. K. G. Wilson, Phys. Rev. 179, 1499 (1969); in Broken Scale Invariance and the Light Cone, Coral Gables Conf. Lectures, eds. M. Dal Cin et al., (Gordon and Breach, New York, 1971) p. 122.
4. D. J. Gross and F. Wilczek, Phys. Rev. D8, 3633 (1973); Ibid D9, 980 (1974); H. Georgi and H. D. Politzer, Phys. Rev. D9, 416 (1974).
5. M. K. Gaillard and B. W. Lee, Phys. Rev. Lett. 33, 108 (1974); G. Altarelli and L. Maiani, Phys. Lett. 52B, 351 (1974).
6. G. Altarelli, K. Ellis, L. Maiani and R. Petronzio, Nucl. Phys. B88, 215 (1975).
7. A. I. Vainshtein, V. I. Zakharov and M. A. Shifman, Zh. ETF (USSR) 72, 1275 (1977) [Sov. Phys. JETP. 45, 670 (1977)]; M. A. Shifman, A. I. Vainshtein and V. I. Zakharov, Nucl. Phys. B120, 316 (1977).
8. H. Galić, D. Tadić and J. Trampetić, Nucl. Phys. B158, 306 (1979); J. F. Donoghue, E. Golowich, W. A. Ponce and B. R. Holstein, Phys. Rev. D21, 186 (1980).

9. J. Ellis, M. K. Gaillard and D. V. Nanopoulos, Nucl. Phys. B100, 313 (1975); N. Cabibbo and L. Maiani, Phys. Lett. 73B, 418 (1978).
10. F. J. Gilman and M. B. Wise, Phys. Rev. D20, 2392 (1979);
B. Guberina and R. D. Peccei, Nucl. Phys. B163, 289 (1980).
11. For a complete list of references see Ref. 2, and M. K. Gaillard, in Weak Interactions - Present and Future, Proc. SLAC Summer Institute 1978, ed. by M. C. Zipf (SLAC, Stanford 1978) p. 397.
12. See, for example, the discussion at the International School of Subnuclear Physics, Erice, Italy, July 1975, in New Phenomena in Subnuclear Physics, ed. by A. Zichichi (Plenum Press, New York 1977) Part A, pp. 489 - 492.
13. S. J. Brodsky and G. P. Lepage, Talk at the XIth Internat. Symp. on Multiparticle Dynamics, Bruges, Belgium, June 1980, and SLAC-PUB-2605 (September 1980) unpublished; A. H. Mueller, Perturbative QCD at High Energies, Columbia University preprint 1980, CU-TP-192, unpublished.
14. The only exception known to the author is a paper by E. Witten¹⁵, in which an elegant technique for such a justification for $\Delta S = 2$ nonleptonic processes (involving the exchange of two W-bosons) was outlined.
15. E. Witten, Nucl. Phys. B122, 109 (1977).
16. Confront, for example, the approaches of Ref. 7 and the works: C. T. Hill and G. G. Ross, Phys. Lett. 94B, 234 (1980); Nucl. Phys. B171, 141 (1980).

17. No "physical intuition" can help to decide whether the form factors in $(\phi^3)_6$ are calculable by the RG analysis. It is just an explicit calculation that shows the failure of the method for this theory and the success, for example, in the calculation of pion form factors in QCD. (For details see Ref. 13.)
18. Hereafter the renormalized sum of QCD corrections to the weak process will be denoted as $\langle \mathcal{H} \rangle$. Non-appearance of external, physical states in such a notation recalls that the calculation of this matrix element is performed at the quark level. Similarly, radiative corrections to the vertex generated by an operator \mathcal{O} will be denoted as $\langle \mathcal{O} \rangle$.
19. Though, of course, the calculability of coefficients depends crucially on the non-Abelian nature of QCD fields.
20. M. B. Wise and E. Witten, Phys. Rev. D20, 1216 (1979).
21. T. Appelquist and J. Carazzone, Phys. Rev. D11, 2856 (1975).
22. W. S. Deans and J. A. Dixon, Phys. Rev. D18, 1113 (1978);
H. Kluberg-Stern and J. B. Zuber, Phys. Rev. D12, 467,482,3159 (1975); S. D. Joglekar and B. W. Lee, Ann. Phys. (N.Y.) 97, 160 (1976).
23. G. Altarelli, G. Curci, G. Martinelli and S. Petrarca, Phys. Lett. 99B, 141 (1981).
24. A. Chodos, R. L. Jaffe, K. Johnson, C. B. Thorn and V. F. Weisskopf, Phys. Rev. D9, 3471 (1974); A. Chodos, R. L. Jaffe, K. Johnson and C. B. Thorn, Phys. Rev. D10, 2599 (1974); T. de Grand, R. L. Jaffe, K. Johnson and J. Kiskis, Phys. Rev. D12, 2060 (1975).

25. N. Isgur and G. Karl, Phys. Lett. 74B, 353 (1978); Phys. Rev. D20, 1191 (1979).
26. The use of the separation indicated in (6.3) was questioned in the following work also:

M. B. Wise, "Strong Effects in Weak Nonleptonic Decays", Ph.D. Dissertation, SLAC-Report-227 (April 1980) p. 95.
27. For example, weak decays of heavy quarkonium might be probably treated by the method similar to those applied in the analysis of strong quarkonium decays in the work A. Duncan and A. Mueller, Phys. Lett. 93B, 119 (1980).

FIGURE CAPTIONS

- Fig. 1. $D^0 \rightarrow K\pi$ process. The interesting part is the weak virtual transition $D^0 \rightarrow \bar{K}^0$. \mathcal{H} denotes the effective weak Hamiltonian.
- Fig. 2. Lowest order corrections to the considered $\Delta C = \Delta S = 1$ process: (x) - a tree diagram; (a) - vertex corrections; (b) box diagrams. The curly line corresponds to the weak boson (W), and the dashed line to the gluon (G).
- Fig. 3. Lowest order corrections to the operator vertices.
- Fig. 4. Higher order corrections to diagrams 2(b).
- Fig. 5. The effect of the differentiation (marked with an X sign). The derivative acts on (a) quark propagators inside the subdiagrams, and (b) external legs of the subdiagrams.
- Fig. 6. The differentiation of an n-loop diagram.
- Fig. 7. $K^0 \rightarrow \pi^+ \pi^-$ decay. The interesting weak transition is enclosed.
- Fig. 8. "Penguin" diagrams, in which the weak transition takes place in a single quark-line.

- Fig. 9. $s \rightarrow d$ transition in the lowest order in weak interactions.
- Fig. 10. $s \rightarrow dG$ transition, related to Fig. 8b.
- Fig. 11. Diagram (a) does not generate new operators. As indicated in (b) it may be related to matrix elements of operators (4.1). In the three-flavor theory only the up-quark contributes in the loop.
- Fig. 12. $\Delta S = \Delta C = 0$ processes. There is no GIM mechanism, and diagrams on the left-hand side generate the penguin operator on the right.
- Fig. 13. Diagrams with a local vertex are, in the course of the regularization, replaced by diagrams with a nonlocal vertex (denoted by a small circle).
- Fig. 14. The scheme for the renormalization.
- Fig. 15. For the certain value of the regularization parameter weak interactions are rediscovered. \mathcal{O} stands for $(\mathcal{O}_{84} + \mathcal{O}_{20})/2$. The result is true in the leading order in M^2 .
- Fig. 16. The regularization procedure in the three-quark theory. \mathcal{P} stands for the operator (4.10).
- Fig. 17. The prototype of a weak transition in a baryon. The effect of the factorization is indicated.

Fig. 18 The factorization for a three-body meson decay.

Fig. 19. The failure of the separability.

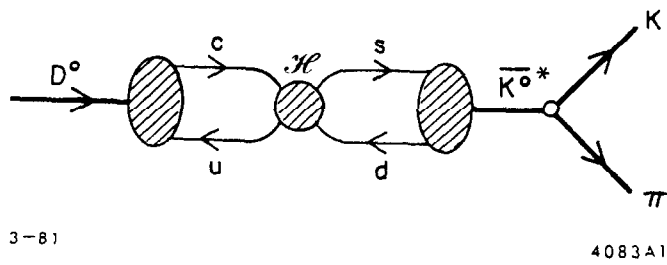
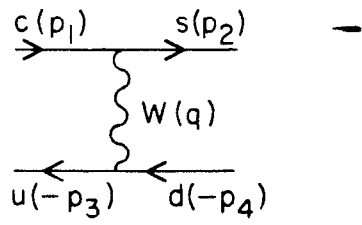
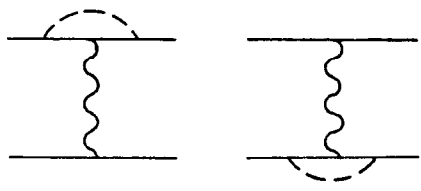


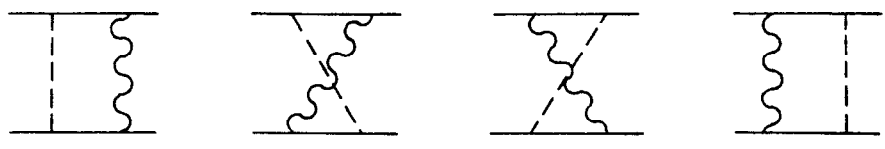
Fig. 1



(x)



(a)



(b)

3-81

4083A2

Fig. 2

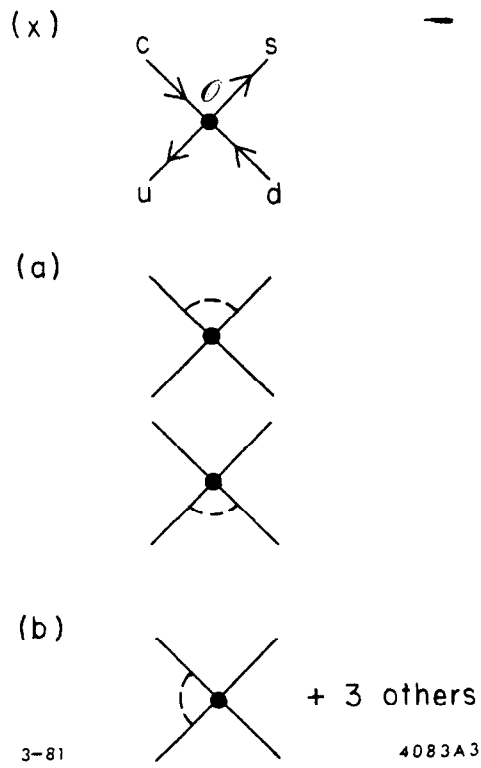
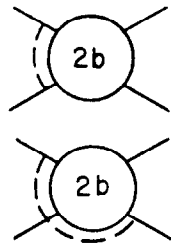
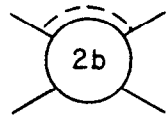
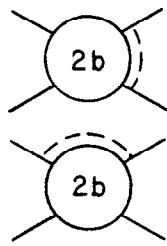


Fig. 3

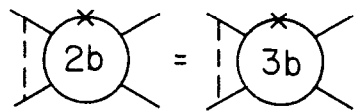


3-81

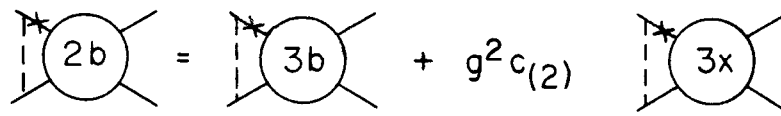


4083A4

Fig. 4



(a)



3-81

(b)

4083A5

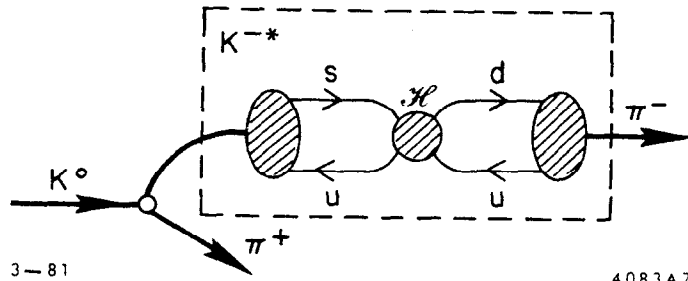
Fig. 5

$$\begin{array}{c}
 \text{Diagram 1} = \text{Diagram 2} + \\
 \sum_{l=1}^k g^{2l} c_{(2l)} \text{Diagram 3}
 \end{array}$$

The diagrammatic equation shows the decomposition of a genus $2k$ surface \mathcal{H}_{2k} into a genus $2k$ surface \mathcal{O}_{2k} plus a sum over l from 1 to k of $g^{2l} c_{(2l)}$ times a genus $2(k-l)$ surface $\mathcal{O}_{2(k-l)}$. Each diagram consists of a central oval with two lines extending from its right side and a vertical dashed line with a star on its left side.

4-81 4083A6

Fig. 6



3-81

4083A7

Fig. 7

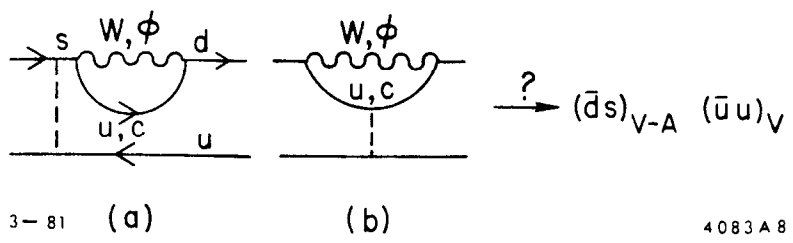


Fig. 8

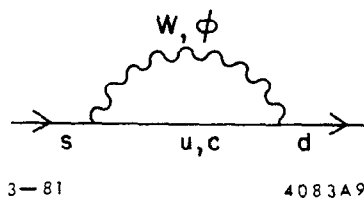
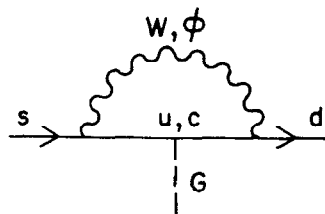


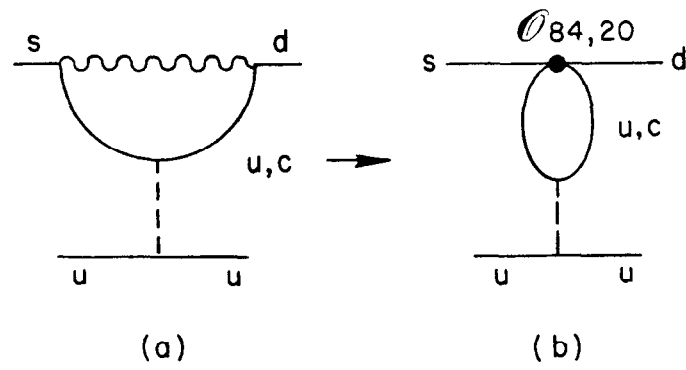
Fig. 9



3-81

4083A10

Fig. 10



3-81

4083A11

Fig. 11

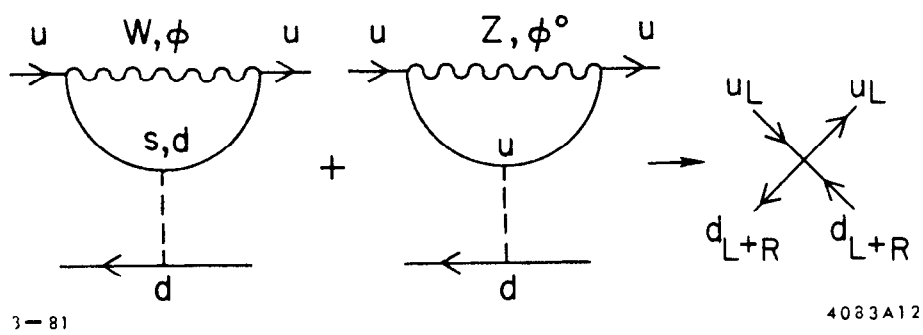


Fig. 12

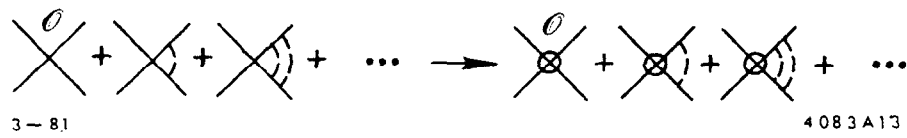


Fig. 13

$$\Lambda^2 \xrightarrow{\text{lim}} \infty \left[\begin{array}{c} \circ \\ \times \end{array} + \begin{array}{c} \circ \\ \times \end{array} + \dots \right]_{p_i p_j} =$$

$$\Lambda^2 \xrightarrow{\text{lim}} \infty \frac{Z^{-1}(\Lambda^2, m_q^2)}{\circ} \times \text{ren} \left[\begin{array}{c} \circ \\ \times \end{array} + \begin{array}{c} \circ \\ \times \end{array} + \dots \right]_{p_i p_j}$$

3-81 4083A14

Fig. 14

$$\left[\begin{array}{c} \text{Diagram 1} \\ \text{Diagram 2} \\ \dots \end{array} \right]_{\Delta^2 = M^2} = -M^2 \left[\begin{array}{c} \text{Diagram 3} \\ \text{Diagram 4} \\ \dots \end{array} \right]$$

The diagram shows a mathematical relationship between two series of Feynman diagrams. The top series, enclosed in large square brackets, consists of three terms: a diagram with a central circle and two diagonal lines crossing at the center, with a small circle above the intersection; a second diagram with a central circle and two diagonal lines, with a dashed arc on the right side; and an ellipsis. Below the right side of these brackets is the label $\Delta^2 = M^2$. To the right of the top series is an equals sign. Below the equals sign is a second series, enclosed in large square brackets, consisting of three terms: a diagram with two horizontal lines and a wavy vertical line between them; a second diagram with two horizontal lines and a dashed vertical line between them; and an ellipsis. To the left of the bottom series is the label $-M^2$.

3-81

4083A15

Fig. 15

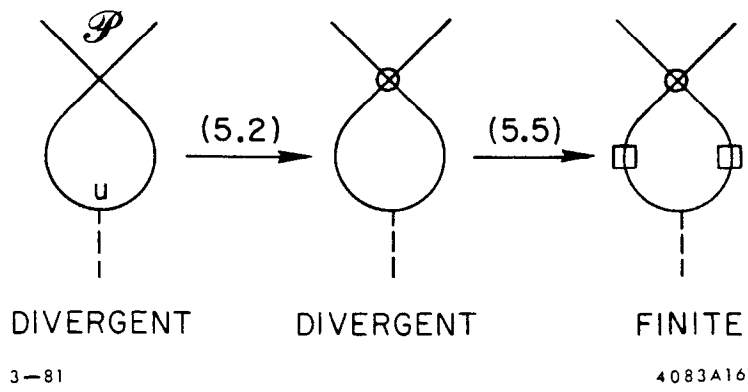


Fig. 16

$$\begin{array}{c}
 \begin{array}{c} \text{---} \\ \text{---} \\ \text{---} \end{array} + \begin{array}{c} \text{---} \\ \text{---} \\ \text{---} \end{array} + \begin{array}{c} \text{---} \\ \text{---} \\ \text{---} \end{array} + \dots = \\
 \\
 C(M) \times \text{ren} \left[\begin{array}{c} \text{---} \\ \text{---} \\ \text{---} \end{array} + \begin{array}{c} \text{---} \\ \text{---} \\ \text{---} \end{array} + \begin{array}{c} \text{---} \\ \text{---} \\ \text{---} \end{array} + \dots \right]
 \end{array}$$

3-81

4083A17

Fig. 17

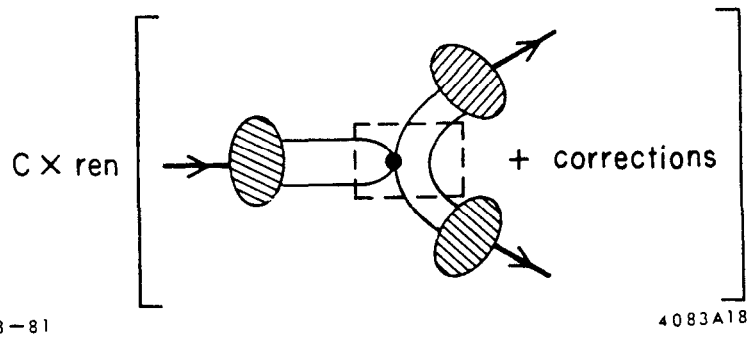
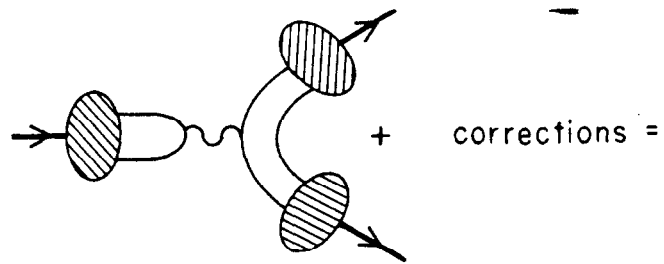


Fig. 18

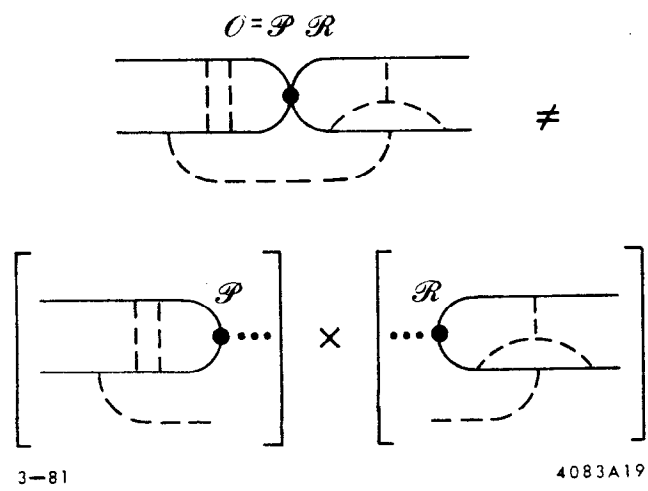


Fig. 19